Supplemental Material for:

Constitutive dysfunction of the Mdm2-p53 axis is linked to premature signs of aging

Authors:
Davor Lessel[1*], Danyi Wu[2*], Carlos Trujillo[3], Thomas Ramezani[4#], Ivana Lessel[1], Mohammad K. Alwasiyah[5], Bidisha Saha[6], Fuki M. Hisama[7], Katrin Rading[1], Ingrid Goebel[1], Petra Schütz[8], Günter Speit[8], Josef Högel[8], Holger Thiele[9], Gudrun Nürnberg[9], Peter Nürnberg[9,10,11], Matthias Hammerschmidt[4,10,11], Yan Zhu[2], David Tong[2], Chen Katz[2], George M. Martin[6,12], Junko Oshima[6,13], Carol Prives[2$], Christian Kubisch[1,8$]

[*]These authors contributed equally to the work.

[$]Correspondence should be addressed to C.K. (c.kubisch@uke.de) or C.P. (clp3@columbia.edu)

Supplemental Text

Bioinformatic filtering of exome sequencing data

Due to the parental consanguinity, we searched for a gene harbouring a very rare or unique homozygous variant with a severe impact on protein structure within the putative linkage regions. We excluded a possible pathogenicity of missense variants in *TRIM45*, *CD48*, *PEX1*, *DGKA*, *INHBC* and *CACNA1G* due to their low evolutionary conservation and the fact that they were predicted benign by Polyphen2 (http://genetics.bwh.harvard.edu/pph2/index.shtml). Mutations in *MYO1A* were initially reported to cause an autosomal dominant form of hearing impairment (1) a symptom which is not present in the index patient. Recently, the pathogenicity of heterozygous *MYO1A* mutations was challenged and it was demonstrated that even homozygous loss of function mutations in *MYO1A* do not cause any overt phenotype (2) so that we also excluded the observed variant in this gene as potentially disease causing. *MCM6, TIMELESS* and *BRCA1* are involved in the maintenance of genomic stability and are thus predicted to lead to chromosomal instability if mutated, at least after treatment with replication-related stressors (3-5). We therefore also excluded variants in these genes as we did not observe genomic instability in primary cell lines of index patient but rather the contrary, i.e. protection against chromosomal instability. In addition, the identified variants in *BRCA1* seem to be rather common polymorphisms in Saudi Arabia (6). *GDE1* knock-out mice (MGI:1891827) are viable and do not display any overt abnormalities apart from reduced glycero-phospho-N-acyl ethanolamine (GP-NAE) phosphodiesterase activity in the brain. Moreover, these mice do not display any signs of premature aging (7). We therefore also excluded the possibility that the variant in *GDE1* may add to the phenotype observed in the index patient. *ARHGAP23* is a still uncharacterized, putative Rho GTPase activating protein of unknown function. Thus, we cannot fully exclude the possibility that the identified variant in this gene may contribute to the observed phenotype. However, the proven dysregulation of the Mdm2-p53 in patient cell lines and the additional functional data presented here strongly suggest that the anti-terminating *MDM2* mutation is responsible for most, if not all of the phenotypes observed in the index patient. Moreover, the *MDM2* mutation was the only alteration with a severe impact on protein structure.

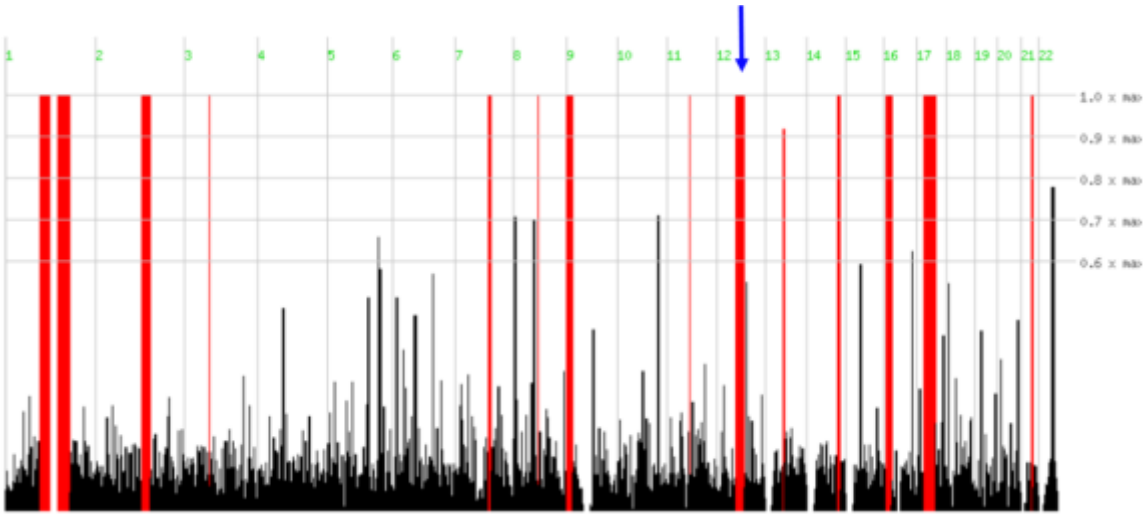

Supplemental Figure S1. Genome-wide homozygosity mapping. Shows the genome-wide homozygosity scores produced by HomozygosityMapper, using 867,266 selected SNP markers from the Affymetrix SNP Array 6.0. These are plotted against the physical position and as a bar chart with red bars indicating the most promising genomic regions. Note 13 extended genomic regions of maximal homozygosity scores. Blue arrow indicates position of MDM2, in one of the largest regions.

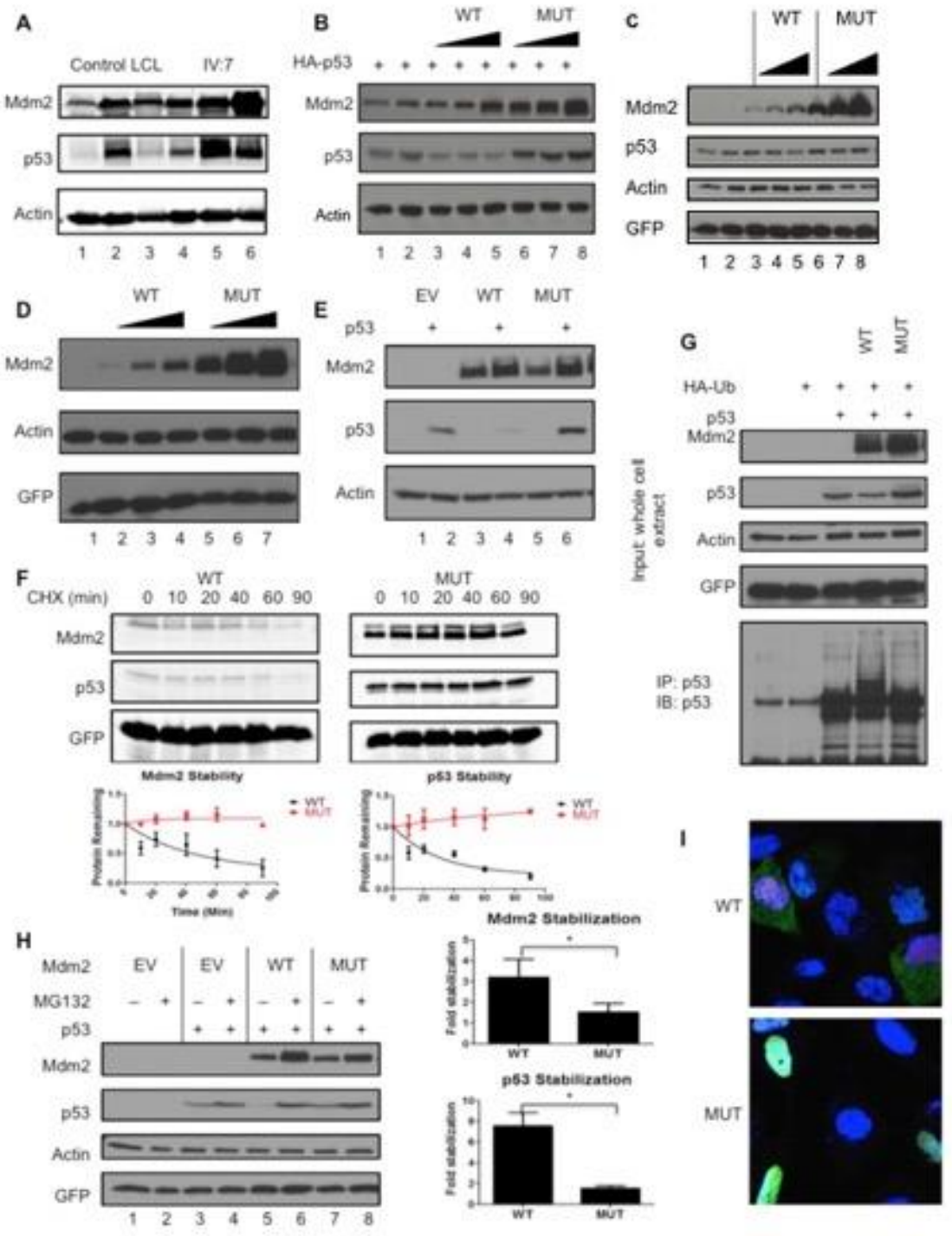

Supplemental Figure S2. Mutated Mdm2 is defective in its ability to regulate p53. (**A**) Levels of Mdm2, p53, and actin in LCLs of an unaffected individual (lanes 1-3: control LCL) and index patient (lanes 4-6: IV:7 LCL). Cell lines were treated with vehicle DMSO (-), Nutlin-3 (N, 10 μM), or daunorubicin (D, 0.1 mg/mL) for 24 hours before harvesting. Cell lysates were used for immunoblotting (IB) with the indicated antibodies (Mdm2: 2A9/3G5/4B11/5B10 mix, p53: MAbs 1801 and DO-1, anti-actin). (**B)** Degradation assay showing levels of ectopically expressed Mdm2 and p53 protein. U2OS cells were

transfected with increasing amounts of constructs expressing N-terminal FLAG-tagged wild-type (WT) and anti-termination mutant (MUT) Mdm2 as indicated (0.5-2 µg) and HA-tagged p53 (200 ng). Cells were harvested at 24 h. Cell lysates were used for immunoblotting (IB) with the indicated antibodies (Mdm2: FLAG; p53: HA, anti-actin). (**C**) Immunoblot showing levels of endogenously expressed p53 in presence of ectopically expressed WT or MUT Mdm2. U2OS cells were transfected with increasing amounts of N-terminal FLAG-tagged Mdm2 WT and MUT constructs as indicated (0.5-2 µg). Cells were harvested at 24h. A GFP construct (50ng) was included as a transfection and loading control. Cell lysates were used for immunoblotting (IB) with the indicated antibodies (Mdm2: FLAG, anti-actin, anti-GFP). (**D**) Levels of Mdm2 protein in a p53-null cell line. H1299 p53-null cells were transfected with increasing amounts of FLAG-tagged Mdm2 WT and MUT constructs as indicated (0.5-2 µg) and harvested at 24h. A GFP construct (50ng) was included as a transfection and loading control. Cell lysates were used for IB with the indicated antibodies (Mdm2: FLAG, anti-actin, anti-GFP). (**E**) Levels of ectopic p53 protein when WT and MUT Mdm2 proteins are expressed at similar levels. U2OS cells were transfected with N-terminal FLAG-tagged Mdm2 constructs calibrated to express equivalent levels of empty vector (EV, 2 µg), WT (2 µg) and MUT (0.4 µg) and HA-tagged p53 (200 ng) as indicated. Expression of GFP (50ng) was included as a transfection and loading control. (**F)** Protein degradation rate of co-expressed Mdm2 and p53 via cylcoheximide chase. U2OS cells were transfected with N-terminal FLAG-tagged Mdm2 WT and MUT constructs (2 µg) and HA-tagged p53 (200ng). 24 hours post-transfection, cells were treated with 100 µg/ml cycloheximide and harvested at the indicated time points. A GFP construct (50 ng) was included as a transfection and loading control. Cell lysates were used for immunoblotting with the indicated antibodies (Mdm2: FLAG, p53: HA, anti-GFP) and polypeptides were quantified using ImageJ software and normalized to GFP. Mdm2 and p53 half-lives were calculated through GraphPad Prism. (**G**) Shows relative ubiquitination of p53 by WT and MUT Mdm2 proteins. H1299 cells were transfected with constructs expressing N-terminal FLAG-tagged WT or MUT Mdm2 (2.6 µg), p53 (260ng), and HA-tagged ubiquitin (866 ng). After 24 h, cells were treated with MG132 (25 µM) for 4h before harvesting. Top panel: Aliquots of transfected cell lysates were subjected to immunoblotting with the indicated antibodies (Mdm2: FLAG, p53: FL-393, anti-GFP) to show input levels of the indicated proteins. Bottom panel: Extracts of cells were immunoprecipitated with anti-p53 antbodies (FL-393) and then probed with the anti-p53 polyclonal antibody (FL-393) to show higher molecular weight ubiquitinated p53 polypeptides. (**H**) Levels of ectopically-expressed Mdm2 and p53 after proteasome inhibition. U2OS cells were transfected with FLAG-tagged Mdm2 constructs calibrated to express equivalent levels of WT (2 µg) or MUT (0.4 µg) and HA-tagged p53 (200 ng). After 24 h, each set was either treated with MG132 (25 µM) for 4h or untreated with fresh media for 4h before harvesting. Left panel: Cell lysates were used for IB with the indicated antibodies. A GFP construct was included as a transfection and loading control. Right panel: Immunoblots were quantified using ImageJ software. Results shown are average of three experiments. Differences in fold of Mdm2 and p53 stabilization when WT or MUT Mdm2 was expressed has $p < 0.05$ significance. (**I**) shows the localization of ectopic p53 in cells expressing WT or MUT Mdm2. U2OS cells were transfected with N-terminal FLAG-tagged Mdm2 WT or MUT constructs (2 µg) and HA-tagged p53 (200 ng). Cells were fixed at 24 h and processed for immunofluorescence as described in Methods. The subcellular localization of p53 was determined using a mouse monoclonal antibody specific for the HA epitope.

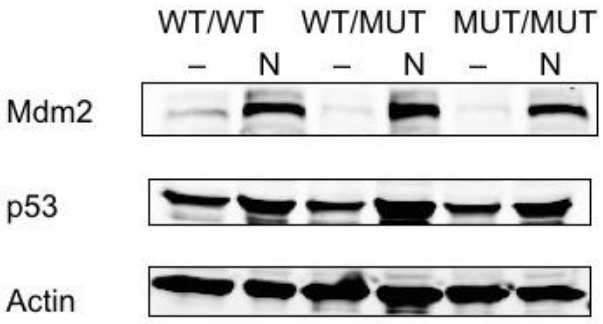

Supplemental Figure S3. **Mdm2 and p53 protein levels in U2OS genome-edited cells.** U2OS genome edited cells expressing WT/WT, WT/MUT, or MUT/MUT Mdm2 were treated with DMSO or Nutlin-3 for 24 hours before harvest and immunoblotting.

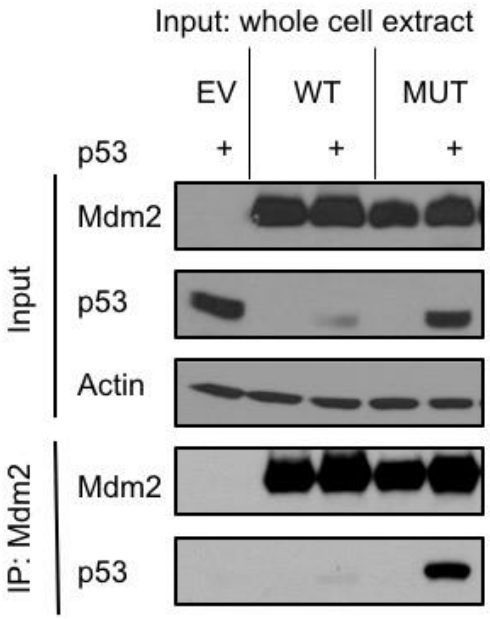

Supplemental Figure S4. Ectopically expressed mutant Mdm2 retains binding to p53. Shows that ectopic Mdm2 can bind to ectopic p53. U2OS cells were transfected with empty vector (EV, 2 µg) or N-terminal FLAG-tagged Mdm2 constructs calibrated to express equivalent levels of WT (2 µg) and MUT (0.35 µg) and harvested at 24 h. Left panel: Aliquots of transfected cell lysates were subjected to immunoblotting with the indicated antibodies (Mdm2: FLAG, p53: HA). Right panel: After co-immunoprecipitation with anti-FLAG antibody and subsequent IB, the proteins were detected using the same antibodies.

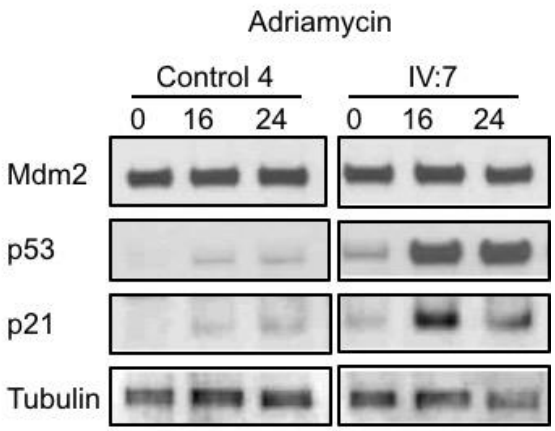

Supplemental Figure S5. Time course of Mdm2, p53 and p21 protein levels after treatment with Adriamycin. Shows protein levels of Mdm2, p53 and p21 of fibroblasts treated with adriamycin (3 μM). Control 88-1 (lanes 1-3) and IV:7 (lanes 4-6) fibroblasts were treated with adriamycin (3 μM) for 24 hours. Cells were harvested either right after treatment (lines 1 and 4), or were further cultured for 16 (lanes 2 and 5) or 24 hours (lanes 3 and 6) in adriamycin free medium. Cell lysates were used for immunoblotting (IB) with Mdm2 (N20), p53 (AF1355), p21 and γ-tubulin. Lanes were run on the same gel but were noncontiguous.

Clinical findings	Patient IV:7	Werner syndrome
Age at presentation	19	> 18
Bilateral cataracts	Absent	+*
Skin changes	+	+*
Pinched nasal bridge	+	+*
Short stature	+	+*
Prematurely gray/thinning hair	+	+*
Parental consanguinity	+	+*
Type 2 diabetes mellitus	-	+
Hypogonadism	+	+
Atherosclerosis	-	+
Neoplasms	-	+
High pitched voice	+	+
Renal failure	+	-

Supplemental Table 1. Clinical findings in the index patient presented here and in Werner syndrome. Skin changes include: scleroderma-like skin changes, tight, atrophic skin changes, hyperpigmentation, skin ulcers. * indicates a cardinal clinical feature for diagnosis of Werner syndrome.

Gene	Chr.	cDNA Change	Protein Change	dbSNP v138	ExAC Browser	Polyphen2
TRIM45	1	c.466C>T	His156Tyr	rs139632476	0/79/115732	benign
CD48	1	c.58T>C	Ser20Pro	rs375107070	0/5/121060	benign
MCM6	2	c.2428T>C	Tyr810His	rs55660827	0/26/121342	possibly damaging
PEX1	7	c.627G>A	Met209Ile	rs200752969	0/19/111150	benign
DGKA	12	c.512G>A	Gly171Asp	**no**	**no**	benign
TIMELESS	12	c.2578C>T	Arg860Cys	**no**	0/1/121406	probably damaging
MYO1A	12	c.1361A>G	Asp454Gly	rs201562120	0/6/117630	probably damaging
INHBC	12	c.361G>A	Asp121Asn	rs201463741	0/5/121140	benign
MDM2	**12**	**c.1492T>C**	**p.*498Qext5**	**no**	**no**	-
GDE1	16	c.242C>T	Thr81Met	**no**	0/1/107830	probably damaging
ARHGAP23	17	c.3047C>T	Thr1016Met	**no**	0/7/21948	possibly damaging
BRCA1	17	c.1648A>C	Asn550His	rs56012641	0/33/121032	probably damaging
BRCA1	17	c.1456T>C	Phe486Leu	rs55906931	0/36/121388	benign
BRCA1	17	c.536A>G	Tyr179Cys	rs56187033	0/33/121410	probably damaging
CACNA1G	17	c.6710C>A	Pro2237His	rs200141555	0/60/117720	benign

Supplemental Table 2. Homozygous variants with minor allele frequencies (MAF) < 0.01 within regions of homozygosity. All alterations were confirmed by Sanger sequencing.

Supplemental references:

1. Donaudy F, et al. Multiple mutations of MYO1A, a cochlear-expressed gene, in sensorineural hearing loss. *American journal of human genetics.* 2003;72(6):1571-7.
2. Eisenberger T, et al. Targeted and genomewide NGS data disqualify mutations in MYO1A, the "DFNA48 gene", as a cause of deafness. *Human mutation.* 2014;35(5):565-70.
3. Ishimi Y. A DNA helicase activity is associated with an MCM4, -6, and -7 protein complex. *The Journal of biological chemistry.* 1997;272(39):24508-13.
4. Urtishak KA, et al. Timeless Maintains Genomic Stability and Suppresses Sister Chromatid Exchange during Unperturbed DNA Replication. *The Journal of biological chemistry.* 2009;284(13):8777-85.
5. Miyoshi Y, et al. Acceleration of chromosomal instability by loss of BRCA1 expression and p53 abnormality in sporadic breast cancers. *Cancer letters.* 2000;159(2):211-6.
6. El-Harith el HA, et al. BRCA1 and BRCA2 mutations in breast cancer patients from Saudi Arabia. *Saudi medical journal.* 2002;23(6):700-4.
7. Simon GM, Cravatt BF. Characterization of mice lacking candidate N-acyl ethanolamine biosynthetic enzymes provides evidence for multiple pathways that contribute to endocannabinoid production in vivo. *Molecular bioSystems.* 2010;6(8):1411-8.